HHS Public Access

Author manuscript

Exp Eye Res. Author manuscript; available in PMC 2024 November 01.

Published in final edited form as:

Exp Eye Res. 2023 November ; 236: 109653. doi:10.1016/j.exer.2023.109653.

A simplified protocol to induce hypoxia in a standard incubator: a focus on retinal cells

Bhavneet Kaur[a], **Bruna Miglioranza Scavuzzi**[a], **Steven F Abcouwer**[a], **David N Zacks**[a]

[a]Department of Ophthalmology and Visual Sciences, Kellogg Eye Center, University of Michigan Medical School, Ann Arbor, MI, USA.

Abstract

Hypoxia chambers have traditionally been used to induce hypoxia in cell cultures. Cellular responses to hypoxia can also be mimicked with the use of chemicals such as cobalt chloride ($CoCl_2$), which stabilizes hypoxia-inducible factor alpha-subunit proteins. In studies of ocular cells using primary cells and cell lines, such as Müller glial cell (MGC) lines, photoreceptor cell lines, retinal pigment epithelial (RPE) cell lines and retinoblastoma cell lines oxygen levels employed in hypoxia chambers range typically between 0.2% and 5% oxygen. For chemical induction of hypoxic response in these cells, the $CoCl_2$ concentrations used typically range from 100 to 600 μM. Here, we describe simplified protocols for stabilizing cellular hypoxia-inducible factor-1α (HIF-1α) in cell culture using either a hypoxia chamber or $CoCl_2$. In addition, we also provide a detailed methodology to confirm hypoxia induction by the assessment of protein levels of HIF-1α, which accumulates in response to hypoxic conditions. Furthermore, we provide a summary of conditions applied in previous studies of ocular cells.

Keywords

Hypoxia chamber; cobalt chloride; hypoxia-inducible factor; retina

1. Introduction

Normal oxygen levels in different body tissues vary significantly (McKeown, 2014). The term “normoxia” describes the typical oxygen partial pressure of O_2 in media surrounding cell cultures under atmospheric oxygen conditions, which is 20.9% oxygen in dry air (Wenger et al., 2015) and depends on factors such as altitude and humidity (Carreau et al., 2011; McKeown, 2014; Wenger et al., 2015). “Hypoxia” describes decreased or insufficient oxygen supply to cells, tissues, or organs, compared to physiological conditions (Carreau et al., 2011; McKeown, 2014; Wenger et al., 2015). The retina is one of the most

Corresponding author: David N. Zacks, MD, PhD, University of Michigan Medical School, Kellogg Eye Center, 1000 Wall St., Ann Arbor, MI 48105, USA, davzacks@med.umich.edu.

Author contributions

Conceptualization and writing: D.Z; Writing—review and editing: B.K, B.M.S and S.F.A. All authors have read and approved the final article.

Declaration of competing interest

The authors declare no conflict of interest.

metabolically active tissues in the body and requires regular and constant oxygen supply for the maintenance of its function (Wangsa-Wirawan and Linsenmeier, 2003).

Conditions such as retinal detachment, diabetes, occlusion of the central retinal artery, or thrombosis of the central retinal vein can compromise oxygenation, leading to the progression of retinal diseases and cell death (Alder et al., 1997; Curtis et al., 2009; Grimm and Willmann, 2012; Kaur et al., 2008; Ross et al., 2022). Retinal detachment (RD) is a serious ocular pathology that occurs when the neurosensory retina becomes separated from the underlying retinal pigmented epithelium (RPE) and the choroid, the vascular layer that provides blood supply and oxygen to the retina. When RD occurs, proper oxygen supply to retinal cells is impaired, leading to hypoxia in the affected area (Piccolino et al., 2005). Hypoxia, in turn, initiates a sequence of pathological events within the retina, encompassing the activation of hypoxia-inducible factor 1-alpha (HIF-1α) and the subsequent upregulation of various stress-related genes, promoting inflammation, augmenting reactive oxygen species (ROS) production, and leading to photoreceptor degeneration (Campochiaro, 2015; Shinojima et al., 2021). In diabetes, for example, chronic hyperglycemia has been shown to damage blood vessels in the retina, leading to vascular constriction and reduced oxygen delivery, even in very early stages of the disease (Alder et al., 1997). This, in turn, prompts the release of vascular endothelial growth factor (VEGF), promoting abnormal blood vessel growth (neovascularization) and increased vascular permeability, exacerbating retinal damage (Aiello et al., 1994).

In cell culture studies, hypoxia chambers have been used to mimic conditions with abnormally limited oxygen supply. A hypoxia chamber provides a controlled environment that allows the effects of specific levels of oxygen to be determined. Designed to fit inside existing laboratory incubators, this self-contained and sealed chamber helps to maintain a hypoxic environment with controlled oxygen levels and a stable temperature. Hypoxic conditions are achieved with specific gas mixtures, generally (1%, 5% or 10% oxygen; with 5% carbon dioxide and the balance nitrogen) (Wu and Yotnda, 2011). In general, oxygen concentrations of less than 2% are considered hypoxic, however, normoxic levels must be considered when selecting the experimental hypoxic conditions (Rinderknecht et al., 2021). An advantage of the use of a hypoxia chamber/incubator is that it is the most natural system to induce cellular hypoxic response, and it permits control of the oxygen fraction in the air surrounding the cultures within it (Rinderknecht et al., 2021). However, it has been shown that if the media is not pre- equilibrated against air containing the lower fraction of O_2, it can take up to 24 hours for the average oxygen concentrations in the cell culture media to stabilize (Newby et al., 2005). It should also be noted that the partial pressure of O_2 at the cell surface not only depends upon the fraction is surrounding air, but also the rate of diffusion to the cells, which typically depends upon the depth of the culture media (if not agitated) and the rate of oxygen consumption of the cells (Al-Ani et al., 2018).

In ocular studies, in addition to the hypoxia incubator/chamber, another commonly employed method for simulating hypoxia is using the hypoxia mimetic cobalt chloride ($CoCl_2$). Compared to the hypoxia chamber, induction of hypoxia with the use of $CoCl_2$ is simple and inexpensive, furthermore, it has the advantage of rapid induction of a cellular response that mimics hypoxia following treatment (Rinderknecht et al., 2021). However,

this method has disadvantages, including possible toxicity and the fact that it does not fully mimic the cellular response to hypoxia, rather, it stabilizes hypoxia-inducible factor alpha proteins (HIF-1α and HIF-2α) (Rinderknecht et al., 2021). The precise mechanism by which $CoCl_2$ stabilizes HIFs is not proven but is likely to involve replacement of ferrous iron(II) by Co^{2+} in the active site of HIF-prolyl hydroxylase enzymes (a.k.a. prolyl hydroxylase domain (PHD) proteins); thus, $CoCl_2$ blocks proline hydroxylation of HIFs, which is the first step in their oxygen-induced polyubiquination and degradation by the proteosome (Muñoz-Sánchez and Chánez-Cárdenas, 2019). In addition, cobalt may inhibit the reduction of ferric iron (Fe^{3+}) to ferrous iron (Fe^{2+}) by ascorbic acid, thus inhibiting PHD activity; and/or Co^{2+} may bind directly to HIF alpha proteins and inhibit their ubiquination (Muñoz-Sánchez and Chánez-Cárdenas, 2019). Importantly, the set of genes induced by hypoxia and $CoCl_2$ treatment may differ, as $CoCl_2$ induction was reported to preferentially activate expression of HIF-1α-responsive genes while inhibiting the expression HIF-2α-responsive genes in hepatic cancer cells (Befani et al., 2013).

Here, we describe general protocols for inducing hypoxia in cell cultures using the hypoxia chamber and $CoCl_2$. In addition, we describe a methodology for assessing protein levels of HIF-1α. Furthermore, we provide a summary of conditions applied to previous studies considering hypoxia chamber/incubator and $CoCl_2$ in ocular cell cultures.

2. Materials and Supplies

2.1. Materials and Supplies for Hypoxia chamber Protocol

2.1.1. Cell culture incubator

2.1.2. Hypoxia chamber

2.1.3. Pre-equilibrated cell culture media*

2.1.4. Two (2) dishes with identical cell cultures prepared with previously equilibrated cell culture media: one will be used as control in the incubator and not in the hypoxia chamber (normoxia); and the other will be placed in the hypoxia chamber within the incubator

2.1.5. Two (2) petri dishes (100 mm) containing 10 mL of sterile water each.

*Preparation: Pre-equilibrated cell culture media can be prepared in several ways: 1. By allowing the culture media to equilibrate under hypoxic conditions in the same hypoxic chamber until the media has reached the desired oxygen concentration, measured by a dissolved oxygen probe. 2. Alternatively, by allowing the culture media to equilibrate in hypoxic conditions in the same hypoxic chamber for at least 24 hours prior to experimental setup. 3. By bubbling nitrogen gas through culture medium, for 15 minutes (for an oxygen level of approximately 1.5%) to 30 minutes (for an oxygen level near 0%) (Newby et al., 2005).

2.2. Materials and Supplies for the use of $CoCl_2$ in stabilizing Hypoxia-Inducible Factor-1α levels

2.2.1. Cobalt (II) chloride hexahydrate, suitable for cell culture. Synonyms: Cobaltous chloride hexahydrate, Cobalt (II) chloride hexahydrate. Formula: $CoCl_2 \cdot 6H_2O$. CAS Number: 7791-13-1. Molecular Weight: 237.93. Soluble in water (100 mg/mL) (Sigma-Aldrich)

2.2.2. Cell culture media

2.2.3. Cell culture incubator

2.2.4. Prepare one culture without the use of $CoCl_2$ to be used as a control.

2.3. Materials and Supplies for the detection of Hypoxia-Inducible Factor-1α (HIF-1α) as a marker of hypoxia

2.3.1. 3-(N-Morpholino)propane sulfonic acid (MOPS)

2.3.2. Ethylene glycol tetraacetic acid (EGTA)

2.3.3. Ethylenediaminetetraacetic acid (EDTA)

2.3.4. Triton x-100

2.3.5. Protease inhibitor mini tablet; ThermoFisher Scientific, Cat #PIA32955

2.3.6. 10x Tris Buffered Saline

2.3.7. Tween-20

2.3.8. Bovine Serum Albumin (BSA)

2.3.9. Human/Mouse/Rat HIF-1 alpha/HIF-1A Antibody; (1:1000) R&D Systems, Cat #MAB15362.

2.3.10. Anti-mouse IgG HRP-linked; (1:8000); GE healthcare Lifesciences, Cat# NA931

2.3.11. Chemiluminescent substrate solution (suggested: SuperSignal West Dura, ThermoFisher)

3. Detailed Methods

3.1. Detailed methods for the use of the Hypoxia chamber

3.1.1. Open the hypoxia chamber, remove lid and trays, and check integrity of the O-ring

3.1.2. Add 2 petri dishes (100 mm) containing 10 mL of sterile water to the chamber base, for maintaining humidity in the chamber.

3.1.3. Place the chamber tray in the chamber and ensure that trays are properly seated in the base.

3.1.4. Place the cell culture dish containing cells into the chamber

3.1.5. Place the lid on the chamber and secure by pushing down

3.1.6. Close the chamber ring clamp, ensuring a hermetic closure of the chamber

3.1.7. Connect the inlet port of the tubing to the hypoxic gas tank, containing the desired hypoxic gas mix (e.g., 1% oxygen, 5% carbon dioxide, balance nitrogen)

3.1.8. Open both the inlet and outlet tubing clamps

3.1.9. Open gas cylinder valve to flush the chamber

3.1.10. Adjust the working output pressure gauge to 2 in mmHg pressure using the pressure adjuster knob, allow the gasflow chamber to completely purge the chamber for ≥8 minutes

3.1.11. Turn off gas flow

3.1.12. Quickly close tubing clamp 1

3.1.13. Quickly close tubing clamp 2

3.1.14. Disconnect the chamber from the gas tank.

Of note, normoxic levels must be considered when selecting the experimental hypoxic conditions. For ocular cells, refer to Table 1 for previously studied conditions.

The pre-equilibration time required for the cell culture medium to reach the desired hypoxic oxygen concentration depends on both the volume of the medium and the target oxygen level. In this experimental protocol, we employ an initial 8-minute hypoxic air purge, followed by a 24-hour period for the pre-equilibration of the cell culture medium before commencing the experiments. Cells were cultured in 4 mL of medium, in 60 mm petri dishes.

Sampling should be performed as quickly as possible, and after sampling or manipulation, the chamber must be re-gassed to restore the desired hypoxic conditions. Allow the chamber to re-equilibrate before further experiments. Modifications to this protocol should be verified by confirming HIF-1α stabilization, as described in item 3.3. Protocol for the detection of Hypoxia-Inducible Factor-1α (HIF-1α) as a marker of hypoxia. It is crucial to maintain consistent hypoxic conditions throughout the cell culture experiments to obtain accurate and reproducible results.

3.2. Detailed methods for the use of $CoCl_2$ in stabilizing Hypoxia Inducible Factor1-α levels

3.2.1. Estimate the final cell culture volume needed

3.2.2. Prepare a 23.793 mM stock solution immediately before use (5.6611 mg/mL) in sterile PBS

3.2.3. Transfer the appropriate volume of stock solution directly to the complete cell culture media to obtain the desired concentration*, adjust according to final desired volume. Refer to table 2 for dilution examples

3.2.4. Plate cells accordingly and transfer cells into regular cell culture incubator.

Of note, when using $CoCl_2$ for the first time, test a range of concentrations to establish non-toxic working concentrations for your cell type and experimental conditions, as this reagent has been demonstrated to reduce cell viability in concentrations as low as 300 μM (Fung et al., 2016; Kuehn et al., 2017; Rodriguez et al., 2021). For ocular cells, employed concentrations typically fall within the range of 50–600 μM. Refer to Table 3 for previously studied conditions in specific cell types.

3.3. Protocol for the detection of Hypoxia-Inducible Factor-1α (HIF-1α) as a marker of hypoxia

3.3.1. Solutions

3.3.1.1. Cell lysis buffer

- Transfer 9.56 mL of Ultrapure water into a 15 mL falcon tube
- Add 200 μL of 1M MOPS
- Add 40 μL of 500 mM EGTA
- Add 100 μL of 0.5 M EDTA
- Add 100 μL of 10% Triton x-100
- Add 1 Thermo Scientific protease inhibitor mini tablet (PIA32955)
- Keep solution on ice during experimental use
- This solution can be aliquoted and stored at −20°C

3.3.1.2. TBS-T

- 100 mL 10x Tris Buffered Saline (TBS)
- 900 mL ultrapure water
- 1 mL Tween-20

3.3.1.3. Blocking buffer

- Weigh 2.5 g of BSA (Bovine Serum Albumin) and transfer into appropriate 50 mL flask
- Add TBS-T solution as described above for a final 50 mL volume
- Mix well
- Maintain refrigerated

3.3.2. Procedure

3.3.2.1. Remove samples from incubator and quickly lyse cells in a solution containing 20 mM MOPS, 2 mM EGTA, 5 mM EDTA, 1% Triton-X-100, 1 mM DTT and protease inhibitors, maintaining samples on ice

3.3.2.2. Centrifuge cell lysates at 16,000 × g in for 10 minutes at 4°C

3.3.2.3. Measure protein concentration in supernatant using preferred methodology (suggested: RC DC Protein Assay Kit, Bio-Rad)

3.3.2.4. Add appropriate volume of preferred loading dye. Keep at room temperature for 25–30 minutes. Suggested loading die: 2x Laemmli Sample Buffer (# 1610737)

3.3.2.5. Load equal amounts of protein (suggested: 20 μg) from each sample into the wells of a 4% to 15%. SDS-PAGE gel and proceed with electrophoresis for protein separation

3.3.2.6. Transfer the protein from gel to a polyvinylidene fluoride membrane

3.3.2.7. Block membrane for 1 hour in Blocking buffer

3.3.2.8. Incubate the membrane overnight with appropriate dilution of the primary antibody (HIF 1-α) in blocking solution. Suggested antibody: Human/Mouse/Rat HIF-1 alpha/HIF-1A Antibody; (1:1000) R&D Systems, Cat #MAB1536

3.3.2.9. Wash the membrane three times for 5–10 minutes each in TBS-T solution

3.3.2.10. Incubate the membrane with appropriate dilution (suggested 1:8000) of the secondary antibody in blocking solution. Suggested antibody: Anti-mouse IgG HRP-linked; (1:8000); GE healthcare Lifesciences, Cat# NA931

3.3.2.11. Wash the membrane three times for 5–10 minutes each in TBS-T solution

3.3.2.12. Add preferred chemiluminescent substrate solution (suggested: SuperSignal West Dura, ThermoFisher)

3.3.2.13. Acquire image

4. Potential Pitfalls and Trouble Shooting

When hypoxia chamber is being used, cell culture media needs to be pre-equilibrated before the start of the experiment, as it may take up to 24 hours for the media to reach hypoxic levels (Newby et al., 2005). Variability in oxygenation levels at the beginning of the experiment may compromise the reproducibility of results. In addition, reoxygenation of cell cultures may occur immediately if the O-ring is compromised, and upon opening of the hypoxia chamber, thus, it is imperative that the chamber remains sealed throughout the duration of the study and opened only at the collection time. If a time-course study is being conducted, the use of additional chambers will be necessary. Ideally, an oxygen analyzer or indicator should be placed in the hypoxia chamber to monitor the maintenance of hypoxic conditions, such as Forensics Detectors, Model: FD-90A-O2. Sample collection should occur as quickly as possible, and samples should be denatured promptly, as oxygen sensing may continue to occur even in the cell lysates (Wenger et al., 2015).

If $CoCl_2$ is used to stabilize hypoxia-inducible factor alpha proteins (HIF-1α and HIF-2α), a range of concentrations should be tested to establish an effective and non-toxic working concentration for your cell type (Rinderknecht et al., 2021). In addition, it is important to note that $CoCl_2$ does not entirely mimic cellular response to hypoxia, thus, caution should be employed when interpreting the results.

Funding

D.N.Z and S.F.A supported by NIH R01EY020823. S.F.A also supported by NIH R01EY029349, NIH R01EY031961 and Research to Prevent Blindness (RPB). B.M.S supported by Training Grant T32AR07080 from the National Institute of Arthritis and Musculoskeletal and Skin Diseases. The work was supported by an NEI Vision Core Research Grant NIH P30EY007003. The content is solely the responsibility of the authors and does not necessarily represent the official views of the National Institutes of Health.

References

Abu El-Asrar A, Ahmad A, Nawaz M, Siddiquei M, De Zutter A, Vanbrabant L, Gikandi P, Opdenakker G, Struyf S, 2022. Tissue Inhibitor of Metalloproteinase-3 Ameliorates Diabetes-Induced Retinal Inflammation. Front Physiol. 12, 1–14. 10.3389/fphys.2021.807747.

Abu El-Asrar A, Nawaz M, Ahmad A, Siddiquei M, Allegaert E, Gikandi P, De Hertogh G, Opdenakker G, 2021. CD146/Soluble CD146 Pathway Is a Novel Biomarker of Angiogenesis and Inflammation in Proliferative Diabetic Retinopathy. Invest Ophthalmol Vis Sci. 62, 1–17. 10.1167/iovs.62.9.32.

Ahmad A, Nawaz M, Siddiquei M, Abu El-Asrar A, 2021. Apocynin ameliorates NADPH oxidase 4 (NOX4) induced oxidative damage in the hypoxic human retinal Müller cells and diabetic rat retina. Mol Cell Biochem. 476, 2099–2109. 10.1007/s11010-021-04071-y. [PubMed: 33515385]

Aiello L, Avery R, Arrigg P, Keyt B, Jampel H, Shah S, Pasquale L, Thieme H, Iwamoto M, Park J, 1994. Vascular endothelial growth factor in ocular fluid of patients with diabetic retinopathy and other retinal disorders. The New England journal of medicine. 331, 1480–1487. 10.1056/NEJM199412013312203. [PubMed: 7526212]

Al-Ani A, Toms D, Kondro D, Thundathil J, Yu Y, Ungrin M, 2018. Oxygenation in cell culture: Critical parameters for reproducibility are routinely not reported. PLoS One. 13, 1–13. 10.1371/journal.pone.0204269.

Alder V, Su E, Yu D, Cringle S, Yu P, 1997. Diabetic retinopathy: early functional changes. Clin Exp Pharmacol Physiol. 24, 785–788. 10.1111/j.1440-1681.1997.tb02133.x. [PubMed: 9315390]

Alivand M, Sabouni F, Soheili Z, 2016. Probable Chemical Hypoxia Effects on Progress of CNV Through Induction of Promoter CpG Demethylation and Overexpression of IL17RC in Human RPE Cells. Curr Eye Res. 41, 1245–1254. 10.3109/02713683.2015.1095933. [PubMed: 26731132]

Alivand M, Soheili Z, Pornour M, Solali S, Sabouni F, 2017. Novel Epigenetic Controlling of Hypoxia Pathway Related to Overexpression and Promoter Hypomethylation of TET1 and TET2 in RPE Cells. J Cell Biochem. 118, 3193–3204. 10.1002/jcb.25965. [PubMed: 28252217]

Alzhrani R, Alhadidi Q, Bachu R, Shah Z, Dey S, Boddu S, 2017. Tanshinone IIA Inhibits VEGF Secretion and HIF-1α Expression in Cultured Human Retinal Pigment Epithelial Cells under Hypoxia. Curr Eye Res. 42, 1667–1673. 10.1080/02713683.2017.1355467. [PubMed: 28937825]

Arjamaa O, Aaltonen V, Piippo N, Csont T, Petrovski G, Kaarniranta K, Kauppinen A, 2017. Hypoxia and inflammation in the release of VEGF and interleukins from human retinal pigment epithelial cells. Graefes Arch Clin Exp Ophthalmol. 255, 1757–1762. 10.1007/s00417-017-3711-0. [PubMed: 28631245]

Bahrami B, Shen W, Zhu L, Zhang T, Chang A, Gillies M, 2019. Effects of VEGF inhibitors on human retinal pigment epithelium under high glucose and hypoxia. Clin Exp Ophthalmol. 47, 1074–1081. 10.1111/ceo.13579. [PubMed: 31265210]

Befani C, Mylonis I, Gkotinakou I, Georgoulias P, Hu C, Simos G, Liakos P, 2013. Cobalt stimulates HIF-1-dependent but inhibits HIF-2-dependent gene expression in liver cancer cells. Int J Biochem Cell Biol. 45, 2359–2368. 10.1016/j.biocel.2013.07.025. [PubMed: 23958427]

Buczek-Thomas J, Rich C, Nugent M, 2019. Hypoxia Induced Heparan Sulfate Primes the Extracellular Matrix for Endothelial Cell Recruitment by Facilitating VEGF-Fibronectin Interactions. Int J Mol Sci. 20, 1–16. 10.3390/ijms20205065.

Campochiaro P, 2015. Molecular pathogenesis of retinal and choroidal vascular diseases. Progress in retinal and eye research. 49, 67–81. 10.1016/j.preteyeres.2015.06.002. [PubMed: 26113211]

Carreau A, El Hafny-Rahbi B, Matejuk A, Grillon C, Kieda C, 2011. Why is the partial oxygen pressure of human tissues a crucial parameter? Small molecules and hypoxia. J Cell Mol Med. 15, 1239–1253. 10.1111/j.1582-4934.2011.01258.x. [PubMed: 21251211]

Chang Y, Lin C, Hsieh M, Wu H, Wu W, Wu W, Kao Y, 2017. High mobility group B1 up-regulates angiogenic and fibrogenic factors in human retinal pigment epithelial ARPE-19 cells. Cell Signal. 40, 248–257. 10.1016/j.cellsig.2017.09.019. [PubMed: 28970183]

Chen Y, Yamada H, Mao W, Matsuyama S, Aihara M, Araie M, 2007. Hypoxia-induced retinal ganglion cell death and the neuroprotective effects of beta-adrenergic antagonists. Brain Res. 1148, 28–37. 10.1016/j.brainres.2007.02.027. [PubMed: 17368577]

Cheng Z, Yao W, Zheng J, Ding W, Wang Y, Zhang T, Zhu L, Zhou F, 2019. A derivative of betulinic acid protects human Retinal Pigment Epithelial (RPE) cells from cobalt chloride-induced acute hypoxic stress. Exp Eye Res. 92–101. 10.1016/j.exer.2018.12.011. [PubMed: 30578788]

Curtis T, Gardiner T, Stitt A, 2009. Microvascular lesions of diabetic retinopathy: clues towards understanding pathogenesis? Eye (Lond). 23, 1496–1508. 10.1038/eye.2009.108. [PubMed: 19444297]

Dougherty C, Smith G, Dorey C, Prentice H, Webster K, Blanks J, 2008. Robust hypoxia-selective regulation of a retinal pigment epithelium-specific adeno-associated virus vector. Mol Vis. 471–480. [PubMed: 18334957]

Du S, Wang S, Wu Q, Hu J, Li T, 2013. Decorin inhibits angiogenic potential of choroid-retinal endothelial cells by downregulating hypoxia-induced Met, Rac1, HIF-1α and VEGF expression in cocultured retinal pigment epithelial cells. Exp Eye Res. 2013, 151–160. 10.1016/j.exer.2013.08.019.

Feng J, Tan W, Li T, Yan Q, Zhu H, Sun X, 2020. Human retinal pigment epithelial cells are protected against hypoxia by BNIP3. Ann Transl Med. 8, 1–12. 10.21037/atm-20-7145. [PubMed: 32055592]

Forooghian F, Razavi R, Timms L, 2007. Hypoxia-inducible factor expression in human RPE cells. Br J Ophthalmol. 91, 1406–1410. 10.1136/bjo.2007.123125. [PubMed: 17567660]

Fuchshofer R, Yu A, Teng H, Strauss R, Kampik A, Welge-Lussen U, 2009. Hypoxia/reoxygenation induces CTGF and PAI-1 in cultured human retinal pigment epithelium cells. Exp Eye Res. 88, 889–899. 10.1016/j.exer.2008.11.036. [PubMed: 19118548]

Fung F, Law B, Lo A, 2016. Lutein Attenuates Both Apoptosis and Autophagy upon Cobalt (II) Chloride-Induced Hypoxia in Rat Műller Cells. PLoS One. 11. 10.1371/journal.pone.0167828.

Golan S, Levi R, Entin-Meer M, Barak A, 2014. The effects of vital dyes on retinal pigment epithelium cells in oxidative stress. Ophthalmic Res. 52, 147–150. 10.1159/000364881. [PubMed: 25300946]

Grimm C, Willmann G, 2012. Hypoxia in the eye: a two-sided coin. High Alt Med Biol. 13, 169–175. 10.1089/ham.2012.1031. [PubMed: 22994516]

Gu Y, Liu W, Liu G, Li X, Lu P, 2021. Assessing the protective effects of cryptotanshinone on CoCl2-induced hypoxia in RPE cells. Mol Med Rep. 24, 1–8. 10.3892/mmr.2021.12379.

Guerra M, Yumnamcha T, Ebrahim A, Berger E, Singh L, Ibrahim A, 2021. Real-Time Monitoring the Effect of Cytopathic Hypoxia on Retinal Pigment Epithelial Barrier Functionality Using Electric Cell-Substrate Impedance Sensing (ECIS) Biosensor Technology. Int J Mol Sci. 22, 1–17. 10.3390/ijms22094568.

Harned J, Nagar S, McGahan M, 2014. Hypoxia controls iron metabolism and glutamate secretion in retinal pigmented epithelial cells. Biochim Biophys Acta. 1840, 3138–3144. 10.1016/j.bbagen.2014.06.012. [PubMed: 24972165]

Henning Y, Blind U, Larafa S, Matschke J, Fandrey J, 2022. Hypoxia aggravates ferroptosis in RPE cells by promoting the Fenton reaction. Cell Death Dis. 13, 1–12. 10.1038/s41419-022-05121-z.

Hollborn M, Ackmann C, Kuhrt H, Doktor F, Kohen L, Wiedemann P, Bringmann A, 2018. Osmotic and hypoxic induction of the complement factor C9 in cultured human retinal pigment epithelial cells: Regulation of VEGF and NLRP3 expression. Mol Vis. 24, 518–535. [PubMed: 30090015]

Hwang S, Seong H, Ryu J, Jeong J, Kang T, Nam K, Seo S, Kim S, Kang S, Han Y, 2020. Phosphorylation of STAT3 and ERBB2 mediates hypoxia induced VEGF release in ARPE 19 cells. Mol Med Rep. 22, 2733–2740. 10.3892/mmr.2020.11344. [PubMed: 32945388]

Ibuki M, Lee D, Shinojima A, Miwa Y, Tsubota K, Kurihara T, 2020 Rice Bran and Vitamin B6 Suppress Pathological Neovascularization in a Murine Model of Age-Related Macular Degeneration as Novel HIF Inhibitors. Int J Mol Sci. 21, 1–25. 10.3390/ijms21238940.

Inoue Y, Shimazawa M, Nakamura S, Imamura T, Sugitani S, Tsuruma K, Hara H, 2014. Protective effects of placental growth factor on retinal neuronal cell damage. J Neurosci Res. 92, 329–337. 10.1002/jnr.23316. [PubMed: 24293397]

Jiang J, Ou W, Luo X, Xiang J, Liu G, Huang S, Li H, He L, Gan J, Han S, Nie C, 2021. Effect of Probenecid on Endothelial Cell Growth Rate and Retinal Angiogenesis in an Oxygen-Induced Retinopathy Model. Front Pharmacol. 12, 1–10. 10.3389/fphar.2021.717351.

Kaur C, Foulds W, Ling E, 2008. Hypoxia-ischemia and retinal ganglion cell damage. Clin Ophthalmol. 2, 879–889. 10.2147/opth.s3361. [PubMed: 19668442]

Kernt M, Thiele S, Liegl R, Kernt B, Eibl K, Haritoglou C, Ulbig M, Kampik A, 2012. Axitinib modulates hypoxia-induced blood-retina barrier permeability and expression of growth factors. Growth Factors. 30, 49–61. 10.3109/08977194.2011.639300. [PubMed: 22168366]

Kiessling E, Peters F, Ebner L, Merolla L, Samardzija M, Baumgartner M, Grimm C, Froese D, 2022. HIF1 and DROSHA are involved in MMACHC repression in hypoxia. Biochim Biophys Acta Gen Subj. 1866, 1–11. 10.1016/j.bbagen.2022.130175.

Klee K, Storti F, Maggi J, Todorova V, Karademir D, Berger W, Samardzija M, Grimm C, 2020. The Expression of Decidual Protein Induced by Progesterone (DEPP) is Controlled by Three Distal Consensus Hypoxia Responsive Element (HRE) in Hypoxic Retinal Epithelial Cells. Genes (Basel). 11. 10.3390/genes11010111.

Kuehn S, Hurst J, Rensinghoff F, Tsai T, Grauthoff S, Satgunarajah Y, Dick H, Schnichels S, Joachim S, 2017. Degenerative effects of cobalt-chloride treatment on neurons and microglia in a porcine retina organ culture model. Exp Eye Res. 155, 107–120. 10.1016/j.exer.2017.01.003. [PubMed: 28089775]

Kunimi H, Lee D, Ibuki M, Katada Y, Negishi K, Tsubota K, Kurihara T, 2021. Inhibition of the HIF-1α/BNIP3 pathway has a retinal neuroprotective effect. FASEB J. 35, 1–17. 10.1096/fj.202100572R.

Kunimi H, Miwa Y, Inoue H, Tsubota K, Kurihara T, 2019. A Novel HIF Inhibitor Halofuginone Prevents Neurodegeneration in a Murine Model of Retinal Ischemia-Reperfusion. Int J Mol Sci. 20, 1–19. 10.3390/ijms20133171.

Kurihara T, Westenskow P, Gantner M, Usui Y, Schultz A, Bravo S, Aguilar E, Wittgrove C, Friedlander M, Paris L, Chew E, Siuzdak G, Friedlander M, 2016. Hypoxia-induced metabolic stress in retinal pigment epithelial cells is sufficient to induce photoreceptor degeneration. Elife. 5, 1–22. 10.7554/eLife.14319.

Lai Y, Hu D, Rosen R, Sassoon J, Chuang L, Wu K, Wu W, 2017. Hypoxia-induced vascular endothelial growth factor secretion by retinal pigment epithelial cells is inhibited by melatonin via decreased accumulation of hypoxia-inducible factors-1α protein. Clin Exp Ophthalmol. 45, 182–191. 10.1111/ceo.12802. [PubMed: 27409056]

Lee D, Miwa Y, Wu J, Shoda C, Jeong H, Kawagishi H, Tsubota K, Kurihara T, 2020. A Fairy Chemical Suppresses Retinal Angiogenesis as a HIF Inhibitor. Biomolecules. 10. 10.3390/biom10101405.

Li K, Zhang Z, Yao J, Zhao Y, Duan J, Cao C, Jiang Q, 2013. Ginsenoside Rg-1 protects retinal pigment epithelium (RPE) cells from cobalt chloride (CoCl2) and hypoxia assaults. PLoS One. 8, 1–9. 10.1371/journal.pone.0084171.

Li N, Gao S, Wang J, Zhu Y, Shen X, 2019. Anti-apoptotic effect of interleukin-17 in a mouse model of oxygen-induced retinopathy. Exp Eye Res. 1–9. 10.1016/j.exer.2019.107743.

Li N, Zhu Y, Wang J, Zhu M, Gao S, Chen Q, Shen X, 2020. Müller cells derived neurotrophin-3 inhibits hypoxia-induced photoreceptor apoptosis via the TrkC/ERK pathway. Cytotechnology. 72, 47–56. 10.1007/s10616-019-00356-9. [PubMed: 31768729]

Liu J, Tang M, Harkin K, Du X, Luo C, Chen M, Xu H, 2020a. Single-cell RNA sequencing study of retinal immune regulators identified CD47 and CD59a expression in photoreceptors-Implications in subretinal immune regulation. J Neurosci Res. 98, 1498–1513. 10.1002/jnr.24618. [PubMed: 32166783]

Liu N, Zhao N, Cai N, 2015. Suppression of the proliferation of hypoxia-Induced retinal pigment epithelial cell by rapamycin through the /mTOR/HIF-1α/VEGF/ signaling. IUBMB Life. 67, 446–452. 10.1002/iub.1382. [PubMed: 25988388]

Liu X, Xie J, Yang L, Li Y, He Y, Liu Z, Zhang Y, Su G, 2020b. Bone marrow mesenchymal stem cells enhance autophagy and help protect cells under hypoxic and retinal detachment conditions. J Cell Mol Med. 24, 3346–3358. 10.1111/jcmm.15008. [PubMed: 32003125]

Long L, Li Y, Yu S, Li X, Hu Y, Long T, Wang L, Li W, Ye X, Ke Z, Xiao H, 2019. Scutellarin Prevents Angiogenesis in Diabetic Retinopathy by Downregulating VEGF/ERK/FAK/Src Pathway Signaling. J Diabetes Res. 2019, 1–17. 10.1155/2019/4875421.

Lu Q, Jiang Y, Qian J, Tao Y, 2013. Apelin-13 regulates proliferation, migration and survival of retinal Müller cells under hypoxia. Diabetes Res Clin Pract. 99, 158–167. 10.1016/j.diabres.2012.09.045. [PubMed: 23332048]

Ma J, Zhu T, Moe M, Ye P, Yao K, 2012. Opticin production is reduced by hypoxia and VEGF in human retinal pigment epithelium via MMP-2 activation. Cytokine. 59, 100–107. 10.1016/j.cyto.2012.03.025. [PubMed: 22534113]

McKeown S, 2014. Defining normoxia, physoxia and hypoxia in tumours-implications for treatment response. Br J Radiol. 87, 1–12. 10.1259/bjr.20130676.

Menegakis A, Klompmaker R, Vennin C, Arbusà A, Damen M, van den Broek B, Zips D, van Rheenen J, Krenning L, Medema R, 2021. Resistance of Hypoxic Cells to Ionizing Radiation Is Mediated in Part via Hypoxia-Induced Quiescence. Cells. 10, 1–23. 10.3390/cells10030610.

Mense S, Sengupta A, Zhou M, Lan C, Bentsman G, Volsky D, Zhang L, 2006. Gene expression profiling reveals the profound upregulation of hypoxia-responsive genes in primary human astrocytes. Physiol Genomics. 25, 435–449. 10.1152/physiolgenomics.00315.2005. [PubMed: 16507782]

Mueller-Buehl A, Buehner T, Pfarrer C, Deppe L, Peters L, Dick B, Joachim S, 2021 Hypoxic Processes Induce Complement Activation via Classical Pathway in Porcine Neuroretinas. Cells. 10, 1–24. 10.3390/cells10123575.

Muñoz-Sánchez J, Chánez-Cárdenas M, 2019. The use of cobalt chloride as a chemical hypoxia model. J Appl Toxicol. 39, 556–570. 10.1002/jat.3749. [PubMed: 30484873]

Nakajima E, David L, Bystrom C, Shearer T, Azuma M, 2006. Calpain-specific proteolysis in primate retina: Contribution of calpains in cell death. Invest Ophthalmol Vis Sci. 47, 5469–5475. 10.1167/iovs.06-0567. [PubMed: 17122138]

Nakajima E, Hammond K, Hirata M, Shearer T, Azuma M, 2017. Contribution of Calpain and Caspases to Cell Death in Cultured Monkey RPE Cells. Invest Ophthalmol Vis Sci. 58, 5412–5420. 10.1167/iovs.17-22325. [PubMed: 29053764]

Newby D, Marks L, Lyall F, 2005. Dissolved oxygen concentration in culture medium: assumptions and pitfalls. Placenta. 26, 353–357. 10.1016/j.placenta.2004.07.002. [PubMed: 15823622]

Peters F, Ebner L, Atac D, Maggi J, Berger W, den Hollander A, Grimm C, 2022. Regulation of ABCA1 by AMD-Associated Genetic Variants and Hypoxia in iPSC-RPE. Int J Mol Sci. 23, 1–20. 10.3390/ijms23063194.

Piccolino F, de la Longrais R, Ravera G, Eandi C, Ventre L, Abdollahi A, Manea M, 2005. The foveal photoreceptor layer and visual acuity loss in central serous chorioretinopathy. American journal of ophthalmology. 139, 87–99. 10.1016/j.ajo.2004.08.037. [PubMed: 15652832]

Produit-Zengaffinen N, Favez T, Pournaras C, Schorderet D, 2016. JNK Inhibition Reduced Retinal Ganglion Cell Death after Ischemia/Reperfusion In Vivo and after Hypoxia In Vitro. Adv Exp Med Biol. 854, 677–683. 10.1007/978-3-319-17121-0_90. [PubMed: 26427475]

Qiao Y, Wang Z, Bunikyte R, Chen X, Jin S, Qi X, Cai D, Feng S, 2021. Cobalt chloride-simulated hypoxia elongates primary cilia in immortalized human retina pigment epithelial-1 cells. Biochem Biophys Res Commun. 555, 190–195. 10.1016/j.bbrc.2021.03.097. [PubMed: 33823365]

Rinderknecht H, Ehnert S, Braun B, Histing T, Nussler AK, Linnemann C, 2021. The Art of Inducing Hypoxia. Oxygen. 1, 46–61. 10.3390/oxygen1010006.

Rodriguez R, Lowe K, Keniry M, Tsin A, 2021. Involvement of TGFβ signaling pathway in oxidative stress and diabetic retinopathy. Arch Clin Exp Ophthalmol. 3, 23–28. [PubMed: 35072165]

Rosen R, Vagaggini T, Chen Y, Hu D, 2015. Zeaxanthin inhibits hypoxia-induced VEGF secretion by RPE cells through decreased protein levels of hypoxia-inducible factors-1α. Biomed Res Int. 2015, 1–11. 10.1155/2015/687386.

Ross B, Jia L, Kong D, Wang T, Yao J, Hager H, Abcouwer S, Zacks D, 2022. Hypoxia-Inducible Factor-1α in Rods Is Neuroprotective Following Retinal Detachment. Invest Ophthalmol Vis Sci. 63, 1–8. 10.1167/iovs.63.11.7.

Saint-Geniez M, Jiang A, Abend S, Liu L, Sweigard H, Connor K, Arany Z, 2013. PGC-1α regulates normal and pathological angiogenesis in the retina. Am J Pathol. 182, 255–265. 10.1016/j.ajpath.2012.09.003. [PubMed: 23141926]

Sant D, Camarena V, Mustafi S, Li Y, Wilkes Z, Van Booven D, Wen R, Wang G, 2018. Ascorbate Suppresses VEGF Expression in Retinal Pigment Epithelial Cells Invest Ophthalmol Vis Sci. 59, 3608–3618. 10.1167/iovs.18-24101. [PubMed: 30025088]

Shelby S, Angadi P, Zheng Q, Yao J, Jia L, Zacks D, 2015. Hypoxia inducible factor 1α contributes to regulation of autophagy in retinal detachment. Exp Eye Res. 137, 84–93. 10.1016/j.exer.2015.06.016. [PubMed: 26093278]

Shinojima A, Lee D, Tsubota K, Negishi K, Kurihara T, 2021. Retinal Diseases Regulated by Hypoxia-Basic and Clinical Perspectives: A Comprehensive Review. J Clin Med. 10. 10.3390/jcm10235496.

Shoda C, Miwa Y, Nimura K, Okamoto K, Yamagami S, Tsubota K, Kurihara T, 2020. Hypoxia-Inducible Factor Inhibitors Derived from Marine Products Suppress a Murine Model of Neovascular Retinopathy. Nutrients. 12, 1–17. 10.3390/nu12041055.

Sigma-Aldrich, SAFETY DATA SHEET. https://www.sigmaaldrich.com/US/en/sds/sigma/c8661 (accessed 03/14/2023).

Sradhanjali S, Tripathy D, Rath S, Mittal R, Reddy M, 2017. Overexpression of pyruvate dehydrogenase kinase 1 in retinoblastoma: A potential therapeutic opportunity for targeting vitreous seeds and hypoxic regions. PLoS One. 12, 1–15. 10.1371/journal.pone.0177744.

Subirada P, Vaglienti M, Joray M, Paz M, Barcelona P, Sánchez M, 2022. Rapamycin and Resveratrol Modulate the Gliotic and Pro-Angiogenic Response in Müller Glial Cells Under Hypoxia. Front Cell Dev Biol. 10, 1–14. 10.3389/fcell.2022.855178.

Sun M, Cherian N, Liu L, Chan A, Aguirre B, Chu A, Strawbridge J, Kim E, Lin M, Tsui I, Gordon L, Wadehra M, 2022. Epithelial membrane protein 2 (EMP2) regulates hypoxia-induced angiogenesis in the adult retinal pigment epithelial cell lines. Sci Rep. 12, 1–13. 10.1038/s41598-022-22696-x. [PubMed: 34992227]

Sun Y, Wen F, Yan C, Su L, Luo J, Chi W, Zhang S, 2021. Mitophagy Protects the Retina Against Anti-Vascular Endothelial Growth Factor Therapy-Driven Hypoxia via Hypoxia-Inducible Factor-1α Signaling Front Cell Dev Biol. 9, 1–14. 10.3389/fcell.2021.727822.

Sweigard J, Matsumoto H, Smith K, Kim L, Paschalis E, Okonuki Y, Castillejos A, Kataoka K, Hasegawa E, Yanai R, Husain D, Lambris J, Vavvas D, Miller J, Connor K, 2015. Inhibition of the alternative complement pathway preserves photoreceptors after retinal injury. Sci Transl Med. 7, 1–23. 10.1126/scitranslmed.aab1482.

Takei A, Ekström M, Mammadzada P, Aronsson M, Yu M, Kvanta A, André H, 2017. Gene Transfer of Prolyl Hydroxylase Domain 2 Inhibits Hypoxia-inducible Angiogenesis in a Model of Choroidal Neovascularization. Sci Rep. 7, 1–14. 10.1038/srep42546. [PubMed: 28127051]

Tamada Y, Fukiage C, Daibo S, Yoshida Y, Azuma M, Shearer T, 2002. Involvement of calpain in hypoxia-induced damage in rat retina in vitro. Comp Biochem Physiol B Biochem Mol Biol. 131, 221–225. 10.1016/s1096-4959(01)00489-4. [PubMed: 11818243]

Tang H, Kong L, Yang Y, Li J, Zou H, 2022. Puerarin suppresses hypoxia-induced vascular endothelial growth factor upregulation in human retinal pigmented epithelial cells by blocking JAK2/STAT3 pathway. Bioengineered. 13, 11636–11645. 10.1080/21655979.2022.2070586. [PubMed: 35510332]

Thakur N, Pandey R, Mehrotra S, 2021. Signal transducer and activator of transcription-3 mediated neuroprotective effect of interleukin-6 on cobalt chloride mimetic hypoxic cell death in R28 cells. Mol Biol Rep. 48, 6197–6203. 10.1007/s11033-021-06586-5. [PubMed: 34318437]

Touhami S, Béguier F, Yang T, Augustin S, Roubeix C, Blond F, Conart J, Sahel J, Bodaghi B, Delarasse C, Guillonneau X, Sennlaub F, 2022. Hypoxia Inhibits Subretinal Inflammation Resolution Thrombospondin-1 Dependently. Int J Mol Sci. 23, 1–12. 10.3390/ijms23020681.

Tsai T, Mueller-Buehl A, Satgunarajah Y, Kuehn S, Dick H, Joachim S, 2020. Protective effect of the extremolytes ectoine and hydroxyectoine in a porcine organ culture. Graefes Arch Clin Exp Ophthalmol. 258, 2185–2203. 10.1007/s00417-020-04854-x. [PubMed: 32710140]

Tsui L, Fong T, Wang I, 2013. The effect of 3-(5'-hydroxymethyl-2'-furyl)-1-benzylindazole (YC-1) on cell viability under hypoxia. Mol Vis. 2260–2273. [PubMed: 24265542]

Udono T, Takahashi K, Nakayama M, Yoshinoya A, Totsune K, Murakami O, Durlu Y, Tamai M, Shibahara S, 2001. Induction of adrenomedullin by hypoxia in cultured retinal pigment epithelial cells. Invest Ophthalmol Vis Sci. 42, 1080–1086. [PubMed: 11274089]

Veltmann M, Hollborn M, Reichenbach A, Wiedemann P, Kohen L, Bringmann A, 2016. Osmotic Induction of Angiogenic Growth Factor Expression in Human Retinal Pigment Epithelial Cells. PLoS One. 11, 1–21. 10.1371/journal.pone.0147312.

Wang H, Geisen P, Wittchen E, King B, Burridge K, D'Amore P, Hartnett M, 2011. The role of RPE cell-associated $VEGF_{189}$ in choroidal endothelial cell transmigration across the RPE. Invest Ophthalmol Vis Sci. 52, 570–578. 10.1167/iovs.10-5595. [PubMed: 20811045]

Wang Y, Sang A, Zhu M, Zhang G, Guan H, Ji M, Chen H, 2016. Tissue factor induces VEGF expression via activation of the Wnt/β-catenin signaling pathway in ARPE-19 cells. Mol Vis. 22, 886–897. [PubMed: 27499609]

Wang Y, Zhang X, Wang X, Wang B, Wang W, 2010. 17-AAG, a Hsp90 inhibitor, attenuates the hypoxia-induced expression of SDF-1alpha and ILK in mouse RPE cells. Mol Biol Rep. 37, 1203–1209. 10.1007/s11033-009-9490-x. [PubMed: 19266313]

Wang Y, Zhou Y, Xiao L, Zheng S, Yan N, Chen D, 2017. E2f1 mediates high glucose-induced neuronal death in cultured mouse retinal explants. Cell Cycle. 16, 1824–1834. 10.1080/15384101.2017.1361070. [PubMed: 28825879]

Wangsa-Wirawan N, Linsenmeier R, 2003. Retinal oxygen: fundamental and clinical aspects. Arch Ophthalmol. 121, 547–557. 10.1001/archopht.121.4.547. [PubMed: 12695252]

Watkins W, McCollum G, Savage S, Capozzi M, Penn J, Morrison D, 2013. Hypoxia-induced expression of VEGF splice variants and protein in four retinal cell types. Exp Eye Res. 116, 240–246. 10.1016/j.exer.2013.09.014. [PubMed: 24076411]

Wenger R, Kurtcuoglu V, Scholz C, Marti H, Hoogewijs D, 2015. Frequently asked questions in hypoxia research. Hypoxia (Auckl). 35–43. 10.2147/HP.S92198. [PubMed: 27774480]

Wu D, Yotnda P, 2011. Induction and testing of hypoxia in cell culture. J Vis Exp. 12, 1–4. 10.3791/2899.

Xie L, Wang Y, Li Q, Ji X, Tu Y, Du S, Lou H, Zeng X, Zhu L, Zhang J, Zhu M, 2021. The HIF-1α/p53/miRNA-34a/Klotho axis in retinal pigment epithelial cells promotes subretinal fibrosis and exacerbates choroidal neovascularization. J Cell Mol Med. 25, 1700–1711. 10.1111/jcmm.16272. [PubMed: 33438362]

Xu W, Wu Y, Hu Z, Sun L, Dou G, Zhang Z, Wang H, Guo C, Wang Y, 2019. Exosomes from Microglia Attenuate Photoreceptor Injury and Neovascularization in an Animal Model of Retinopathy of Prematurity. Mol Ther Nucleic Acids. 16, 778–790. 10.1016/j.omtn.2019.04.029. [PubMed: 31163320]

Yamagishi R, Aihara M, 2014. Neuroprotective effect of astaxanthin against rat retinal ganglion cell death under various stresses that induce apoptosis and necrosis. Mol Vis. 20, 1796–1805. [PubMed: 25593507]

Yamagishi R, Aihara M, Araie M, 2011. Neuroprotective effects of prostaglandin analogues on retinal ganglion cell death independent of intraocular pressure reduction. Exp Eye Res. 93, 265–270. 10.1016/j.exer.2011.06.022. [PubMed: 21791206]

Yamamoto T, Kanda A, Kase S, Ishida S, 2021. Hypoxia Induces Galectin-1 Expression Via Autoinduction of Placental Growth Factor in Retinal Pigment Epithelium Cells. Invest Ophthalmol Vis Sci. 62, 1–12. 10.1167/iovs.62.2.22.

Yang Q, Tripathy A, Yu W, Eberhart C, Asnaghi L, 2017. Hypoxia inhibits growth, proliferation, and increases response to chemotherapy in retinoblastoma cells. Exp Eye Res. 162, 48–61. 10.1016/j.exer.2017.07.001. [PubMed: 28689747]

Yang Y, Wu J, Lu W, Dai Y, Zhang Y, Sun X, 2022. Olaparib, a PARP-1 inhibitor, protects retinal cells from ocular hypertension-associated oxidative damage. Front Cell Dev Biol. 10, 1–16. 10.3389/fcell.2022.925835.

Yoon C, Kim D, Kim S, Park G, Hur D, Yang J, Park S, Kim Y, 2014. MiR-9 regulates the post-transcriptional level of VEGF165a by targeting SRPK-1 in ARPE-19 cells. Graefes Arch Clin Exp Ophthalmol. 252, 1369–1376. 10.1007/s00417-014-2698-z. [PubMed: 25007957]

Youale J, Bigot K, Kodati B, Jaworski T, Fan Y, Nsiah N, Pappenhagen N, Inman D, Behar-Cohen F, Bordet T, Picard E, 2022. Neuroprotective Effects of Transferrin in Experimental Glaucoma Models. Int J Mol Sci. 23, 1–18. 10.3390/ijms232112753.

Zhang H, Li T, Cai X, Wang X, Li S, Xu B, Wu Q, 2020. MicroRNA-203a-3p regulates CoCl2-induced apoptosis in human retinal pigment epithelial cells by targeting suppressor of cytokine signaling 3. J Diabetes Complications. 34, 1–8. 10.1016/j.jdiacomp.2020.107668.

Zhang J, Zhao J, Bai Y, Huang L, Yu W, Li X, 2015. Effects of p75 neurotrophin receptor on regulating hypoxia-induced angiogenic factors in retinal pigment epithelial cells. Mol Cell Biochem. 398, 123–134. 10.1007/s11010-014-2212-2. [PubMed: 25200140]

Zhang P, Zhang X, Hao X, Wang Y, Hui Y, Wang H, Hu D, Zhou J, 2009. Rac1 activates HIF-1 in retinal pigment epithelium cells under hypoxia. Graefes Arch Clin Exp Ophthalmol. 247, 633–639. 10.1007/s00417-008-1031-0. [PubMed: 19165496]

Zhang X, Feng Z, Li C, Zheng Y, 2012. Morphological and migratory alterations in retinal Müller cells during early stages of hypoxia and oxidative stress. Neural Regen Res. 7, 31–35. 10.3969/j.issn.1673-5374.2012.01.005. [PubMed: 25806055]

Zhang Y, Zhao L, Wang L, Yang X, Zhou A, Wang J, 2018. Placental growth factor promotes epithelial-mesenchymal transition-like changes in ARPE-19 cells under hypoxia. Mol Vis. 24, 340–352. [PubMed: 29769799]

Zhang Z, Wang Y, Shi Y, Hou H, Zhang C, Cai Y, Dou G, Yao L, Li F, 2011. Hypoxia specific SDF-1 expression by retinal pigment epithelium initiates bone marrow-derived cells to participate in Choroidal neovascularization in a laser-induced mouse model. Curr Eye Res. 36, 838–849. 10.3109/02713683.2011.593107. [PubMed: 21851170]

Zhao J, Geng Y, Hua H, Cun B, Chen Q, Xi X, Yang L, Li Y, 2015. Fenofibrate inhibits the expression of VEGFC and VEGFR-3 in retinal pigmental epithelial cells exposed to hypoxia. Exp Ther Med. 10, 1404–1412. 10.3892/etm.2015.2697. [PubMed: 26622498]

Zheng F, Jang W, Fung F, Lo A, Wong I, 2016. Up-Regulation of ENO1 by HIF-1α in Retinal Pigment Epithelial Cells after Hypoxic Challenge Is Not Involved in the Regulation of VEGF Secretion. PLoS One. 11, 1–12. 10.1371/journal.pone.0147961.

Zhou Q, Zhou L, Qian J, Yuan Z, Chen Z, 2018. NKILA inhibition protects retinal pigment epithelium cells from hypoxia by facilitating NFκB activation. Biochem Biophys Res Commun. 503, 3134–3141. 10.1016/j.bbrc.2018.08.105. [PubMed: 30144973]

Zhu M, Liu X, Wang S, Miao J, Wu L, Yang X, Wang Y, Kang L, Li W, Cui C, Chen H, Sang A, 2016. PKR promotes choroidal neovascularization via upregulating the PI3K/Akt signaling pathway in VEGF expression. Mol Vis. 22, 1361–1374. [PubMed: 27994435]

Zhu M, Wang Y, Zhu L, Du S, Wang Z, Zhang Y, Guo Y, Tu Y, Song E, 2022. Crosstalk Between RPE Cells and Choroidal Endothelial Cells via the ANXA1/FPR2/SHP2/NLRP3 Inflammasome/Pyroptosis Axis Promotes Choroidal Neovascularization. Inflammation. 414–427. 10.1007/s10753-021-01555-3. [PubMed: 34595678]

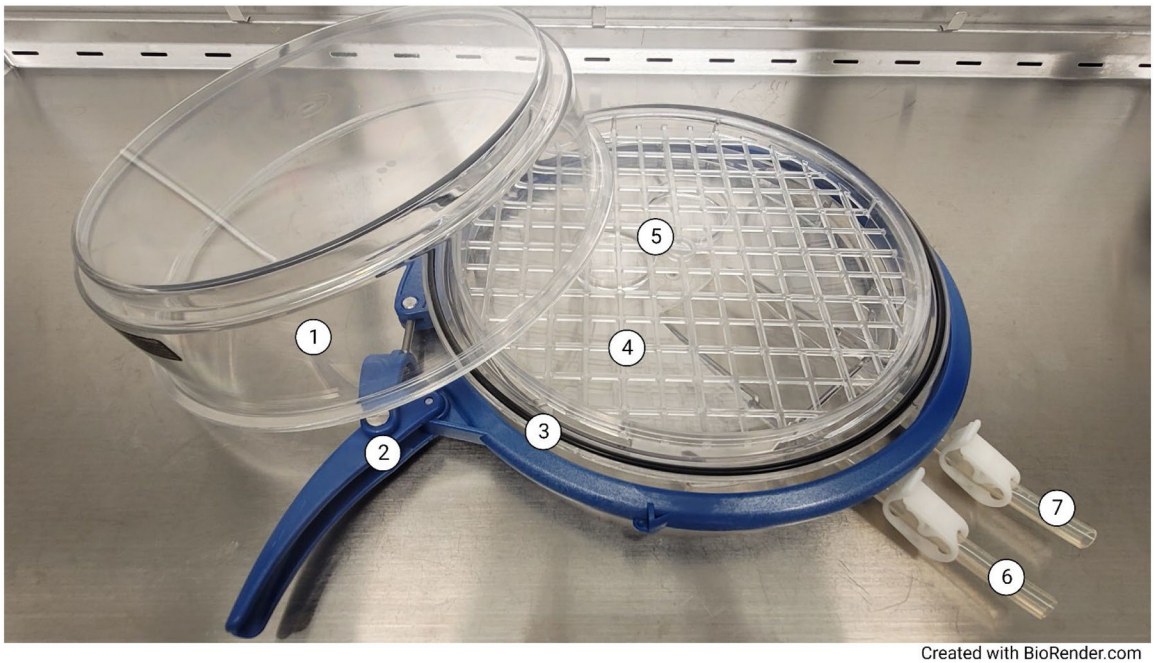

Figure 1.

Hypoxia chamber parts (**1**) Chamber lid; (**2**) Ring clamp; (**3**) O-ring; (**4**) Chamber tray; (**5**) Petri dishes containing sterile water; (**6**) Inlet tubing with clamp; (**7**) Outlet tubing with clamp.

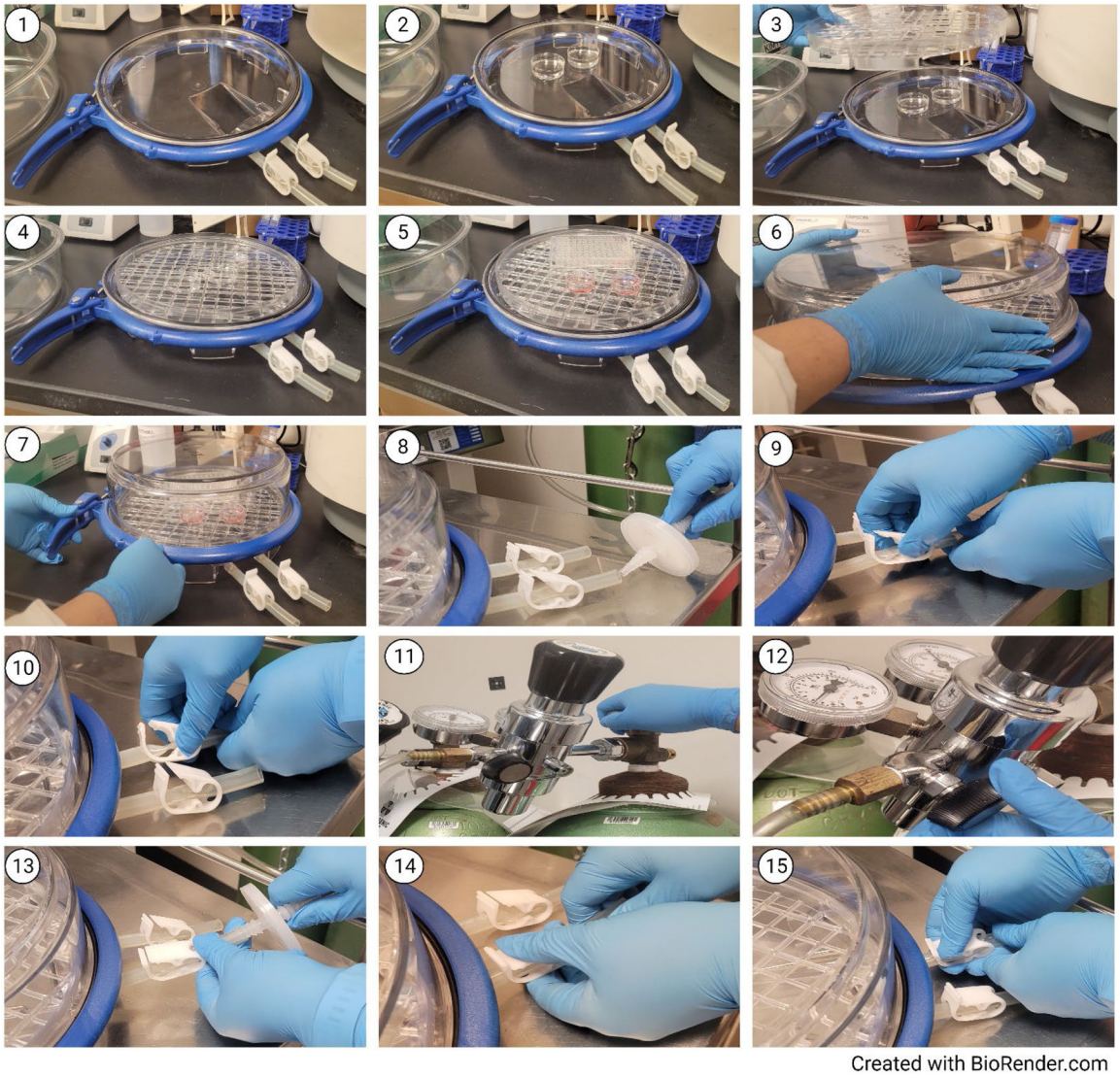

Figure 2.

Schematic protocol for the use of the hypoxia chamber. (**1**) Open the hypoxia chamber; (**2**) Add petri dishes containing of sterile water to the chamber base; (**3**) Identify the correct position of the chamber tray; (**4**) Add the chamber tray, making sure it is secured in place; (**5**) Add the cell cultureware containing one of the twin cultures in the chamber; (**6**) Add the chamber lid; (**7**) Close the chamber ring clamp, ensuring a hermetical closure of the chamber; (**8**) Connect the chamber to the hypoxic gas tank; (**9**) Open first tubing clamp; (**10**) Open second tubing clamp; (**11**) Open gas cylinder valve to flush the chamber; (**12**) Adjust the working output pressure gauge to 2 in.Hg pressure using the pressure adjuster knob, allowing the chamber to purge for 8 minutes; (**13**) Turn off gas flow; (**14**) Quickly close tubing clamp 1; (**15**) Quickly close tubing clamp 2; (16) Disconnect the chamber from the gas tank.

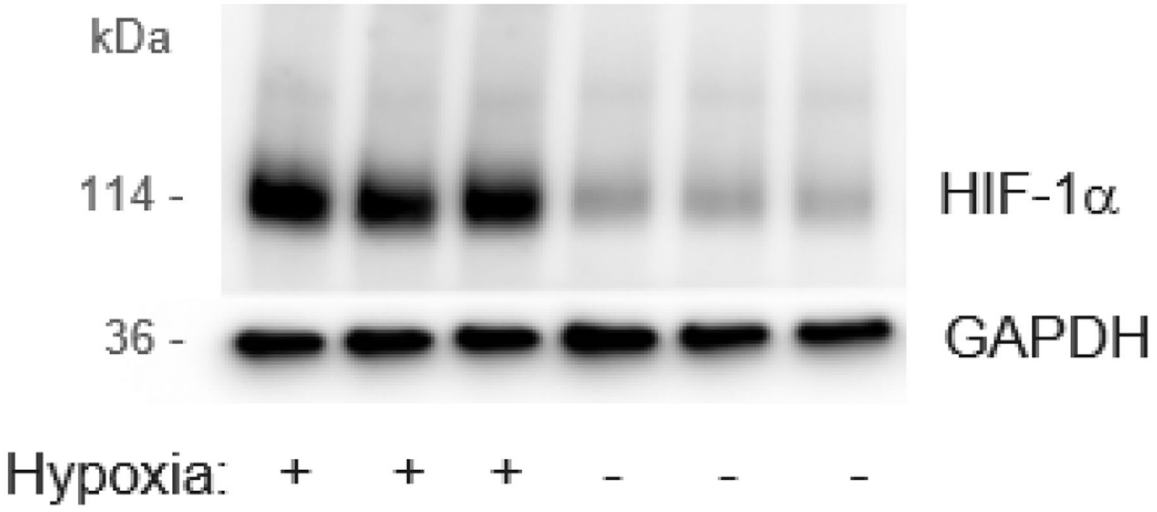

Figure 3.
Western blot of HIF-1α protein in mouse immortalized cone photoreceptor cell line 661W, after 24 hours of incubation in hypoxia chamber (5%Carbon dioxide, 1%Oxygen, balance Nitrogen).

Table 1.

Summary of studies employing low oxygen levels for evaluating optical cells.

Cell/tissue type	Species	% Oxygen	Reference
661W cell line	Mouse	0.2%	(Kiessling et al., 2022)
661W cell line	Mouse	0.5%	(Tsui et al., 2013)
661W cell line	Mouse	1%	(Inoue et al., 2014; Kunimi et al., 2021; Kunimi et al., 2019; N Li et al., 2019; N Li et al., 2020; X Liu et al., 2020b; Shelby et al., 2015; Y Sun et al., 2021; Sweigard et al., 2015; Xu et al., 2019)
661W cell line	Mouse	3%	(Produit-Zengaffinen et al., 2016)
661W cell line	Mouse	5%	(J Liu et al., 2020a)
Astrocytes	Human	1%	(Mense et al., 2006)
Astrocytes	Rat	<0.7%	(Watkins et al., 2013)
Fetal retinal pigment epithelial cells (hfRPE)	Human	1%	(H Wang et al., 2011)
Fetal retinal pigmented epithelial cells (RPE), F-0202	Human	1%	(Udono et al., 2001)
induced pluripotent stem cell (iPSC)-derived RPE cells (iRPEs) iPSC-RPE	Human	4%	(Peters et al., 2022)
Müller cells	Rat	<0.7%	(Watkins et al., 2013)
Müller cells	Mouse	1%	(N Li et al., 2019; N Li et al., 2020)
Müller glial cell (MGC) line MIO-M1	Human	0%#	(Saint-Geniez et al., 2013)
Müller glial cell (MGC) line MIO-M1	Human	1%	(Subirada et al., 2022; Y Sun et al., 2021)
Retina (cultured)	Monkey	0%*	(Nakajima et al., 2006)
Retina (cultured)	Rat	0%*	(Tamada et al., 2002)
Retinal endothelial cells (HRECs)	Human	0.2%	(Klee et al., 2020)
Retinal Ganglion Cell (RGC) - Primary	Rat	5%	(Chen et al., 2007; Yamagishi and Aihara, 2014; Yamagishi et al., 2011)
Retinal microvascular endothelial cells (RMEC)	Rat	<0.7%	(Watkins et al., 2013)
Retinal pigment epithelial (RPE) cell line ARPE-19	Human	0%*	(Xie et al., 2021; Zheng et al., 2016)
Retinal pigment epithelial (RPE) cell line ARPE-19	Human	0.2%	(Klee et al., 2020)
Retinal pigment epithelial (RPE) cell line ARPE-19	Human	<0.25%	(Zhou et al., 2018)
Retinal pigment epithelial (RPE) cell line ARPE-19	Human	0.5%	(Harned et al., 2014; Sradhanjali et al., 2017; M Sun et al., 2022)
Retinal pigment epithelial (RPE) cell line ARPE-19	Human	1%	(Arjamaa et al., 2017; Dougherty et al., 2008; Hwang et al., 2020; Kunimi et al., 2019; Shoda et al., 2020; Takei et al., 2017; Tang et al., 2022; Udono et al., 2001; Yoon et al., 2014; J Zhang et al., 2015; Zhu et al., 2022)
Retinal pigment epithelial (RPE) cell line ARPE-19	Human	2%	(Golan et al., 2014)
Retinal pigment epithelial (RPE) cell line ARPE-19	Human	3%	(Forooghian et al., 2007; Henning et al., 2022)
Retinal pigment epithelial (RPE) cell line D407	Human	1%	(Feng et al., 2020; NN Liu et al., 2015; Tang et al., 2022; Udono et al., 2001)
Retinal pigment epithelial (RPE) cell line HRPEpiC	Human	0.2%	(Klee et al., 2020)

Cell/tissue type	Species	% Oxygen	Reference
Retinal pigment epithelial (RPE) cell line hTERT RPE1	Human	1%	(Menegakis et al., 2021; Yamamoto et al., 2021)
Retinal pigmented epithelial cells (RPE)	Human	1%	(Buczek-Thomas et al., 2019; Fuchshofer et al., 2009; Hollborn et al., 2018; Kernt et al., 2012; Ma et al., 2012; Rosen et al., 2015; P Zhang et al., 2009)
Retinal pigmented epithelial cells (RPE)	Human	3%	(Kurihara et al., 2016)
Retinal pigmented epithelial cells (RPE)	Monkey	≤1%	(Nakajima et al., 2017)
Retinal pigmented epithelial cells (RPE)	Mouse	3%	(Kurihara et al., 2016)
Retinal pigmented epithelial cells (RPE)	Porcine	2%	(Touhami et al., 2022)
Retinal pigmented epithelial cells (RPE)	Rat	<0.7%	(Watkins et al., 2013)
Retinal Cell Line (R28)	Rat	0.2%	(Y Yang et al., 2022)
Retinoblastoma cell lines (Y79 and Weri-Rb1)	Human	0.5%	(Sradhanjali et al., 2017)
Retinoblastoma cell lines (Y79 and Weri-Rb1)	Human	1%	(Q Yang et al., 2017)

*Treatment described as 95% N_2 and 5% CO_2

#Treatment described as complete deprivation of oxygen or anoxia

Table 2.

Examples of 23.793 mM $CoCl_2$ stock solution dilutions into 10 mL of cell culture media.

Desired final $CoCl_2$ concentration (μM)	Stock Volume (μL)	Stock concentration	Final cell culture media volume
50	21.01	23.793 mM	10 mL
100	42.03		
200	84.06		
250	105.07		
300	126.09		
350	147.10		
400	168.12		
500	210.15		
600	252.18		

Table 3.

Summary of studies employing cobalt chloride to induce hypoxia in optical cells.

Cell type	Species	Dose	Reference
661W cell line	Mouse	200 μM	(Kunimi et al., 2019; Lee et al., 2020)
661W cell line	Mouse	300 μM	(Rodriguez et al., 2021)
Endothelial cells	Human	150 μM	(Jiang et al., 2021)
Müller cells	Rabbit	250 mM	(Lu et al., 2013)
Müller cells	Rat	500 μM	(X Zhang et al., 2012)
Müller glial cell line MIO-M1	Human	250 μM	(Ahmad et al., 2021)
Müller glial cell line MIO-M1	Human	300 μM	(Abu El-Asrar et al., 2021)
Müller glial cell line MIO-M1	Human	75 μM - 500 μM	(Subirada et al., 2022)
Retina	Mouse	200 μM	(Y Wang et al., 2017)
Retina	Porcine	300 μM	(Mueller-Buehl et al., 2021 ; Tsai et al., 2020)
Retinal endothelial cells (HRECs)	Human	200 μM	(Long et al., 2019)
Retinal Ganglion Cell (RGC) - Primary	Rat	100 μM	(Youale et al., 2022)
Retinal microvascular endothelial cells (HRMECs)	Human	300 μM	(Abu El-Asrar et al., 2022)
Retinal Müller glial cells	Human	300 μM	(Abu El-Asrar et al., 2022)
Retinal pigmented epithelial cells (RPE)	Human	100 μM	(Ma et al., 2012)
Retinal pigmented epithelial cells (RPE)	Human	100 – 350 μM	(Alivand et al., 2016; Alivand et al., 2017)
Retinal pigmented epithelial cells (RPE)	Human	150 μM	(Hollborn et al., 2018; Rosen et al., 2015)
Retinal pigmented epithelial cells (RPE)	Human	200 μM	(ZX Zhang et al., 2011)
Retinal pigmented epithelial cells (RPE)	Human	8 mM, 12 mM	(Cheng et al., 2019)
Retinal pigmented epithelial cells (RPE)	Mouse	200 μM	(YQ Wang et al., 2010)
Retinal pigment epithelial (RPE) cell line ARPE-19	Human	10 – 1000 μM	(Guerra et al., 2021)
Retinal pigment epithelial (RPE) cell line ARPE-19	Human	50 – 300 μM	(Y Wang et al., 2016)
Retinal pigment epithelial (RPE) cell line ARPE-19	Human	100 μM	(Du et al., 2013; Hwang et al., 2020; Sant et al., 2018)
Retinal pigment epithelial (RPE) cell line ARPE-19	Human	100 – 1000 μM	(Chang et al., 2017)
Retinal pigment epithelial (RPE) cell line ARPE-19	Human	150 μM	(Alzhrani et al., 2017; Lai et al., 2017; Veltmann et al., 2016)
Retinal pigment epithelial (RPE) cell line ARPE-19	Human	200 μM	(Bahrami et al., 2019; Ibuki et al., 2020 ; Kunimi et al., 2019; Shoda et al., 2020; Takei et al., 2017; H Zhang et al., 2020; Y Zhang et al., 2018; Zhao et al., 2015; Zhu et al., 2016)
Retinal pigment epithelial (RPE) cell line ARPE-19	Human	200 – 800 μM	(Gu et al., 2021)
Retinal pigment epithelial (RPE) cell line ARPE-19	Human	300 μM	(Zheng et al., 2016)
Retinal pigment epithelial (RPE) cell line ARPE-19	Human	600 μM	(Zhou et al., 2018)
Retinal pigment epithelial (RPE) cell line ARPE-19	Human	600 μM	(KR Li et al., 2013)
Retinal pigment epithelial (RPE) cell line ARPE-19	Human	8 mM	(Cheng et al., 2019)
Retinal pigment epithelial (RPE) cell line hTERT RPE1	Human	25 – 75 μg/mL	(Qiao et al., 2021)
Retinal pigment epithelial (RPE) cell line hTERT RPE1	Human	75 μg/mL	(Qiao et al., 2021)

Cell type	Species	Dose	Reference
Retinal Cell Line (R28)	Human	0.5 mM	(Thakur et al., 2021)
Retinoblastoma cell lines (Y79 and Weri-Rb1)	Human	50 – 400 μM	(Q Yang et al., 2017)
Retinoblastoma cell lines (Y79 and Weri-Rb1)	Human	100 – 300 μM	(Sradhanjali et al., 2017)